Journal of Fluorescence (2018) 28:1281–1294
https://doi.org/10.1007/s10895-018-2278-4

ORIGINAL ARTICLE

Synthesis and Evaluation of a Schiff-Based Fluorescent Chemosensors for the Selective and Sensitive Detection of Cu^{2+} in Aqueous Media with Fluorescence Off-On Responses

Maria Sadia[1] · Robina Naz[1] · Jehangir Khan[1] · Rizwan Khan[1]

Received: 7 May 2018 / Accepted: 9 August 2018 / Published online: 15 September 2018

Abstract

Copper being an essential nutrient; also pose a risk for human health in excessive amount. A simple and convenient method for the detection of trace amount of copper was employed using an optical probe **R1** based on Schiff base. The probe was synthesized by Schiff base condensation of benzyl amine and 2-hydroxy-1-napthaldehyde and characterized by single X-ray diffraction, ^{1}H NMR and FTIR. By screening its fluorescence response in a mixture of DMSO and H_2O (20:80, *v/v*) **R1** displayed a pronounced enhancement in fluorescence only upon treatment with copper. Other examined metal ions such as alkali, alkaline and transition had no influence. Within a wide pH range 5–12 **R1** could selectively detect copper by interrupting ICT mechanism that results in CHEF. From Job's plot analysis a 2:1 binding stoichiometry was revealed. The fluorescence response was linear in the range 1–10×10^{-9} M with detection limit 30×10^{-9} M. Association constant was determined as 1×10^{11} M^{-2} by Benesi-Hilderbrand plot. As a fast responsive probe it possesses good reproducibility and was employed for detection of copper in different water samples.

Keywords Fluorescent chemosensor · Schiff base · Copper · CHEF · Real-time detection

Introduction

In the last few years, the development of fast, cheap and efficient fluorescent chemosensors with high sensitivity and selectivity for the detection of heavy and transition metal ions such as Cu^{2+}, Cd^{2+}, Pb^{2+}, and Hg^{2+} has attracted wide-spread interests of chemists, environmentalists, clinical biochemists and biologists because of their fundamental role in biological, environmental and medicinal application [1–6].

Fluorescent chemosensors typically consist of two parts: ionophore (metal chelator) and fluorophore (signaling unit). The two parts are interconnected through a proper spacer. Ionophore is required for analyte binding and as a result of metal binding, photophysical properties of the fluorophore such as fluorescence intensity, lifetime of the excited state or absorption wavelength changes, achieving the purpose of identification [7–9].

✉ Maria Sadia
mariasadia@gmail.com

[1] Department of Chemistry, University of Malakand, Chakdara, Lower Dir, KPK, Pakistan

Among the metal ions, after zinc and iron, copper is the third most abundant vital trace element for life that plays an important role in various fundamental physiological and biological processes in organisms [10]. It is also a toxic chemical that is not biodegradable and bioaccumulative and can accumulate in food chain or human through uptake or consumption and may be hazardous to human health or the environment [11]. Copper is present in sediments, natural water, and in the other medium such as air and soil. Industrial effluent are the potential source of copper contamination such as waste water from industries manufacturing fungicides, fertilizers, bactericides, algaecides, electronic goods, copper plumbing, as well as the use of copper as a mordant for textile dyes, as an activator in froth floatation of sulfide ores and in plating by products. Natural sources also contribute to the contamination of copper that include sea spray, forest fires, decaying vegetation, volcanoes and windblown. [12–14]. Due to these extensive industrial applications copper can be a significant environmental pollutant of worldwide concern [15].

Copper is also an essential micronutrient in the human body. Because of its redox-active nature it acts as an essential cofactor of many enzymes such as tyrosinase, cytochrome c oxidase and superoxide dismutase [16]. It is necessary for the development of bone, nerve coverings, and connective tissue [17].

Copper exist in three common oxidation states Cu^{2+} (cupric ion), Cu^{+} (cuprous ion) and Cu^{0} (metal). Among the three species the most commonly occurring and toxic to living organism is the cupric ion. Copper possess high affinity for the ligand containing sulfur and nitrogen donors thus it effects enzymes whose activities depend on amino and sulhydryl groups [18]. Due to its toxicity at cellular level, its distribution and homeostasis is highly controlled by various factors including chaperones and copper transport proteins. Abnormal level of copper can cause various problems and disorders. For example, under overloading condition copper can cause disorders such as allergies, migraine headaches, anxiety, depression, anorexia, premenstrual syndrome, fatigue, kidneys and blood problems, Wilson's, Parkinson's, Alzheimer's and prion diseases in humans and its deficiency is associated with myelopathy. In living cells uncontrolled reaction of copper ion with oxygen result in the production of ROS (reactive oxygen species) that can damage proteins, nucleic acid and lipids Excessive absorption of Cu^{2+} also effects the growth of plants including fewer leaves, shortening of root length and decrease in the plants biomass [19–22]. According to World Health Organization (WHO), the permissible limit of copper in drinking water is 2 ppm (30 μM) or 1.5 mg/L [23, 24]. In view of such toxic effects of copper, efficient detection of trace amount of copper in environmental water samples is very necessary. For these reasons, great effort has been dedicated to design fluorescent chemosensors for specific recognition and detection of copper.

Chelation enhanced fluorescent type chemosensor are more sensitive to metal ions as compared to Chelation enhanced quenching chemosensors. Cu^{2+} is known as a fluorescence quencher and most of the fluorescent chemosensors reported for copper so far, detection of copper occur through a fluorescence quenching process that undergoes a charge or energy transfer mechanism and "turn-on" fluorescent sensors for recognition of copper are still rare. Thus, there is a great demand to develop "turn-on" fluorescent chemosensors for specific and sensitive detection of copper [25–27].

Schiff base derivatives have attracted much attention as an optical chemosensor for the detection of the metal ions because of their structural flexibility, excellent applicability, high selectivity, high efficiency and simplicity of synthetic mode. Schiff base compounds form strong complexes with transition metal ions. For the Schiff base to be used as a fluorescent sensor, the presence of a strong fluorophore is required. Schiff base compounds incorporating π- conjugated fluorescent fragment are extensively used as fluorescent chemosensor for the metal ions [28–31].

It was within our interests to design a CHEF type Schiff-base fluorescent sensor for selective detection of copper ion. Therefore we designed and develop a new fluorescent probe for copper ion named as (E)-1 ((benzylimino)methyl)naphthalen-2-ol (**R1**). The synthesis was simple, single step the product was highly selective towards copper ion. **R1** exhibited very weak fluorescence due to ICT mechanism which was inhibited upon interaction with copper ion and enhancement of fluorescence was observed. The proposed fluorescent chemosensors contain two parts naphthalene group which is the signaling moiety acting as a fluorophore and imine and hydroxyl group are the binding sites acting as a receptor. We select 2-Hydroxynaphthalene as a fluorophore because of its cheap cost, good binding sites, competitive stability in the environment and characteristic photophysical properties such as low fluorescence quantum yield and short fluorescence lifetime [32, 33].

Experimental

Materials and Instrumentation

2-hydroxy-1-napthaldehyde, Benzyl amine, Dimethyl sulfoxide (DMSO), Hydrochloric acid 37%, Sodium hydroxide, Acetone, and salts of Cu^{2+}, Na^{+}, Mg^{2+}, K^{+}, Zn^{2+}, Mn^{2+}, Hg^{2+}, Ba^{2+}, Pb^{2+}, Ni^{2+}, Cd^{2+}, Ni^{2+}, Co^{2+}, As^{3+}, Fe^{3+} and Ce^{3+} were purchased from commercial sources and were used without further purification. Throughout all experiments distilled water was used. pH adjustments were made by using HCl or NaOH. To minimize the release of cations in the solution and their sorption, the glassware's were first washed with acid and then rinsed with distilled water. For fluorometric determination of Cu^{2+} optically four sides' clear quartz cuvettes were used and were washed with acetone before use.

The ^{1}H NMR spectra of the samples were obtained on Bruker Avance 400 MHz. spectrometer. For FTIR spectra samples were prepared as KBr pallets and the spectrum was obtained on FTIR spectrophotometer Pretige 21 Shimadzu Japan in the region 400–4000 cm^{-1}. X-ray structure analysis of the sample was conducted using Bruker kappa APEXIICCD diffractometer. For the measurement of melting points a Bicote Stuart-SMP 10 Japan was used. UV–vis absorption spectroscopy measurements were conducted on UV-visible 1800 spectrophotometer. The emission spectra were monitored using fluorescence spectrophotometer RF 5301 PC Shimadzu Japan equipped with fluorescence free quartz cuvettes of 1 cm path length. Slit width were 5 nm both for excitation and emission and a steady state 150 W Xenon lamp was used as an excitation source. The pH of the test solution was monitored by a BANTE instrument pH meter. All measurements were conducted at room temperature.

Synthesis of Chemosensor R1

R1 was prepared according to the published method [34, 35]. The synthetic route of **R1** is shown in the Scheme 1.2-hydroxy-1- napthaldehyde 10 mmol (1.7218 g) was dissolved in 10 mL methanol and after adding few drop of acetic acid, it was boiled for a while. After 5 min methanolic solution of

Scheme 1 Synthetic route of chemosensor **R1**

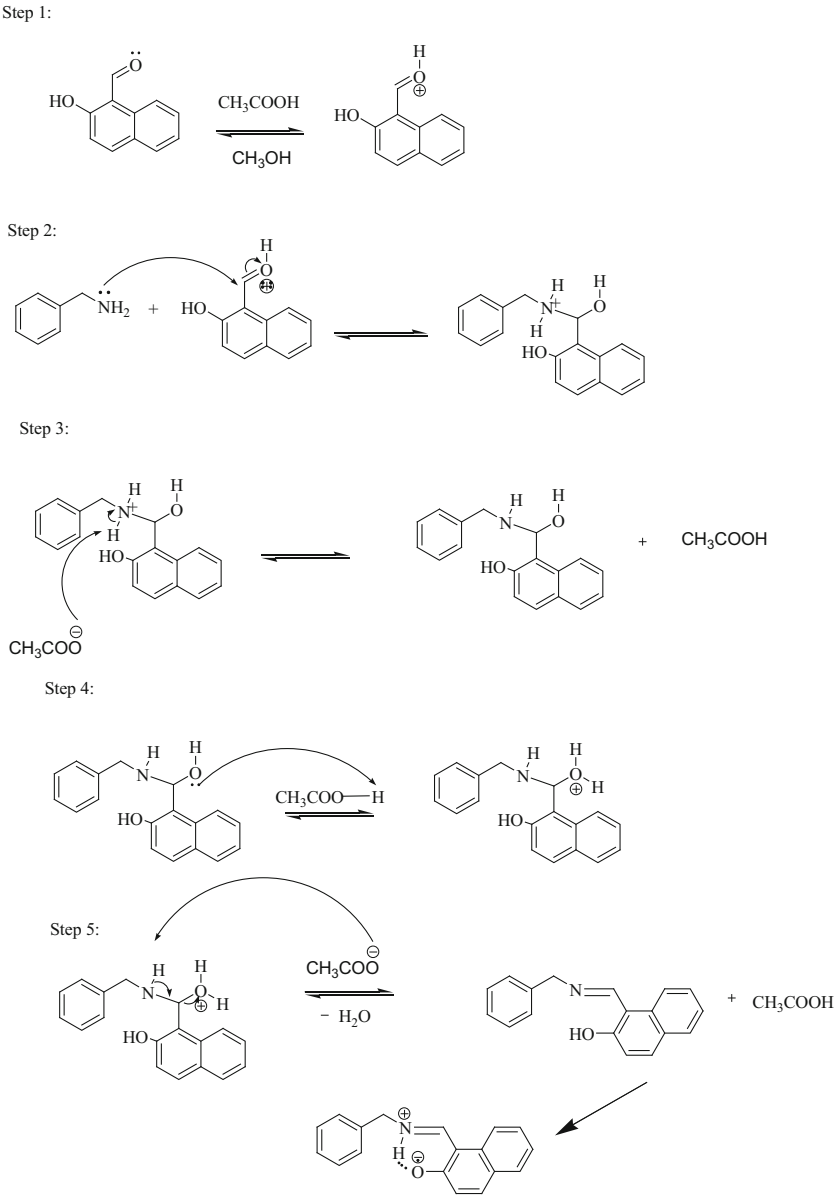

benzylamine 10 mmol (1.09 mL) was slowly added to it drop wise. The mixture was refluxed for about 12 h at 80 °C to give a clear yellow solution. To get the crystal, solvent was evaporated slowly at room temperature by keeping the solution in air for several days. After evaporation of the solvent rod shaped yellow color single crystal were obtained which were recrystallized from ethanol. Yield 80%, mp 120–122 °C, IR (KBr, cm^{-1}): $\nu_{C\text{-}OH}$, 1296, 1207; $\nu_{C=N,}$ 1614, $\nu_{aromaticC=C,}$ 1492, 1435; $\nu_{aromatic\text{-}C\text{-}H,}$ 3035. ^{1}HNMR (400 MHz, DMSO): δ14.5 s (NHO), 9–10s (-N=CH, 1H), 7.7–8.2d (H-naphtha, 2H), 6.0–8.0 m (ArH, 9H), 4.5–5.0 s ($ArCH_2$, 2H).

General Information

Melting point was determined in open mouth capillary and uncorrected. For spectroscopic investigation analytical reagent

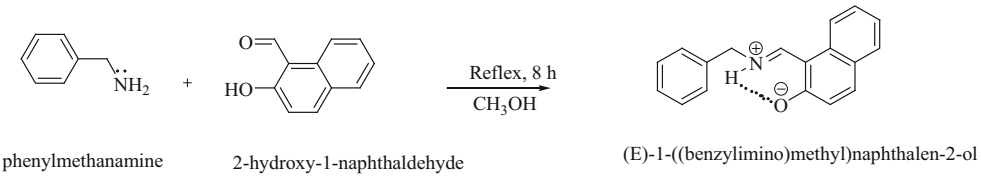

phenylmethanamine 2-hydroxy-1-naphthaldehyde (E)-1-((benzylimino)methyl)naphthalen-2-ol

Scheme 2 Chemical structure and synthesis of (E)-1-((benzylimino)methyl)naphthalen-2-ol

Table 1 FTIR spectral frequencies for chemosensor R1

IR-band (C=N) cm^{-1}	IR-band (C-OH) cm^{-1}	IR-band aliphatic (-C-O) cm^{-1}	IR-band aromatic (-C-H) cm^{-1}	IR-band aromatic (C=C) cm^{-1}
1614	1296, 1207	1138, 1038	3035	1492, 1435

grade DMSO and distilled water were used. Fluorescence and absorption spectra of the chemosensor **R1** was recorded in DMSO:H20 (20:80) at room temperature. Fluorescence-sensing property of the chemosensor **R1** towards metal ions was conducted using sulphate salt of Cu^{2+}, Mg^{2+}, Zn^{2+}, Mn^{2+}; nitrate salt of Pb^{2+}, Ba^{2+}, Cd^{2+}, K^{+}, Ce^{3+}, Hg^{2+}; bromide salt of Co^{2+}; chloride salt of Na^{+}, Ni^{2+}, Fe^{3+} and oxide of As^{3+}. For pH adjustment HCL and NaOH were used. From the fluorescence intensity data association constant was determined by Benesi-Hilderbrand Plot. The excitation and emission wavelength were 320 and 645 nm respectively. All the measurements were conducted at room temperature.

Results and Discussion

Synthesis and Characterization

Chemosensor **R1** was obtained with good yield by condensing 2-hydroxy-1- napthaldehyde with benzylamine in methanol as shown in scheme 2 and it was well characterized by FTIR, ^{1}H NMR and single X-ray crystallography and spectroscopic tools.

Characterization by FTIR

In order to determine the functional group in the synthesized Schiff-based fluorescent chemosensor **R1** FTIR spectroscopy was conducted and the data is given in the Table 1.

In the region 400–4000 cm^{-1} several absorption bands were observed in the FTIR spectrum of the chemosensor **R1**. Assignments of characteristics bands correspond to various functional groups present in the chemosensor were made by comparison method. The FTIR spectrum confirms the formation of imine bond (-C=N) and no band assigned to (C=O) was detected. Thus, the disappearance of carbonyl (-C=O) peak in the region of 1700 cm^{-1} and appearance of the (-C=N) peak in the region of 1614 cm^{-1} confirms the formation of chemosensor **R1**. The band at 3035 cm^{-1} corresponds to the stretching vibration of aromatic-C-H. The spectrum exhibit absorption band at 1492, 1435 and at 1296, 1207 cm^{-1} typically of aromatic-C=C and phenolic-O-H stretching vibration. The bands at 1138 and 1038 cm^{-1} correspond to aliphatic-C-O [36–38].

Characterization by Single Crystal X-Ray Diffraction

The synthesis of chemosensor **R1** was a single-step straight forward reaction and no side products were observed or isolated during the course of reaction. From reaction mixtures, by slow evaporation of the solvent crystals were separated, Suitable for single X-ray diffraction analysis. Crystallographic measurement were carried outs with Bruker kappa APEXIICCD diffractometer, with graphite-monochromator (Mo-kα radiation (λ = 0.71073° A) at ambient temperature. For data collection ωscan and multi-scan correction were applied. The crystal structure solution and refinements of chemosensor **R1** were

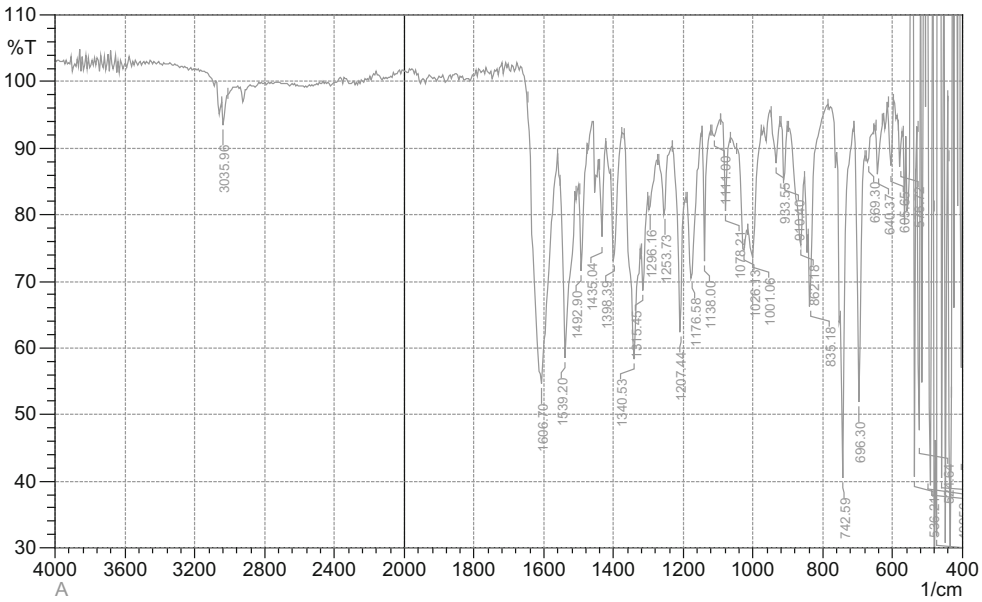

Fig. 1 FTIR spectrum of the chemosensor **R1**

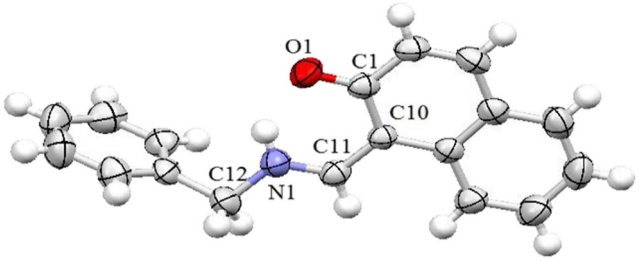

Fig. 2 Molecular structure of chemosensor **R1** with partial numbering scheme

handled with SHELXL-97 [39] and *publ CIF* [40]. Full-matrix least-squares techniques were done for final refinement on F2. The molecular view of chemosensor **R1** with partial numbering scheme is shown in Figs. 1 and 2. The crystallographic data reveals to crystal structure of chemosensor **R1** and relevant refinement parameters are given in Table 2 and the selected bond angles and bond lengths are listed in Table 2.

The crystal of R1 is mono-clinic crystal system with space group $P2_1/n$. In the crystal amine moiety through 84.74° is twisted with respect to naphthalene moiety. Around N_1 the geometry is trigonal planner, demonstrating that the lone pair of nitrogen is involved in conjugation without disturbing sp^2 hybridization. The bond distance between N_1-C_{11} is 1.295 Å which is comparable with the double bond character of C=N bond and bond length of N_1-C_{12} is 1.464 Å and C_1-O is 1.267 Å. X-ray diffraction map revealed that imine-N is bonded with H and exists as –C=NH^+– and O of phenolic –OH as O^- which is identical with similar reported structure [33]. Intramolecular hydrogen bonding stabilized the structure as shown in the Fig. 3.

Characterization by ^{1}H NMR

The ^{1}HNMR spectrum of the chemosensor R1 displays a proton at δ14.5 which shows the interaction of imine nitrogen with the OH proton resulting in zwitter ion as shown in the Fig. 4. A singlet proton at δ9–10 attributed to -N=CH represents the imine group (Schiff base). Similarly two doublet protons exhibited at δ7.7–8.2 are assigned for the naphthalene. Further aromatic group protons at δ6.0–8.0 represent the benzene and naphthalene rings. A pair of singlet protons at δ4.5–5.0 are assigned for the $ArCH_2$.

Table 2 Crystallographic data and details of refinements for chemosensor **R1**

Crystal	R1
Empirical formula, Formula weight	$C_{18}H_{15}NO$, 261.31
Crystal system, Space group	Monoclinic, $P2_1/c$
Temperature (K)	296
a, b, c, (Å)	25.391 (4), 6.5797 (11), 8.1779 (13)
β (°)	92.277 (9)
V (Å^3)	1365.2 (4)
Z	4
Radiation type	Mo $K\alpha$
μ (mm^{-1})	0.08
Crystal	Yellow, crystal size (0.42 × 0.30 × 0.26)
Data collection	
Diffractometer, scan mode	Bruker kappa APEXIICCD, Multi-scan and ωscan
No of measured, independent and observed [$I \geq 2\sigma(I)$] reflections	5051, 2746, 1772
R_{int}	0.040
$(\sin \theta/\lambda)_{max}$ (Å^{-1})	0.651
Refinements	
R [$F^2 > 2\sigma(F^2)$], wR (F^2), S	0.050, 0.126, 0.96
No. of reflections	2746
No. of restraints	2
H-atom treatment	H-atom parameter constrained
$\Delta\rho_{max}$, $\Delta\rho_{min}$ (e Å^{-3})	0.16, −0.17
Absolute structure	Flack x determined using 598 quotients [(I+)-(I-)]/[(I+) + (I-)] (Parsons, Flack and Wagner, Acta Cryst. B69 (2013) 249–259)
Absolute structure parameter	−0.7 (10)

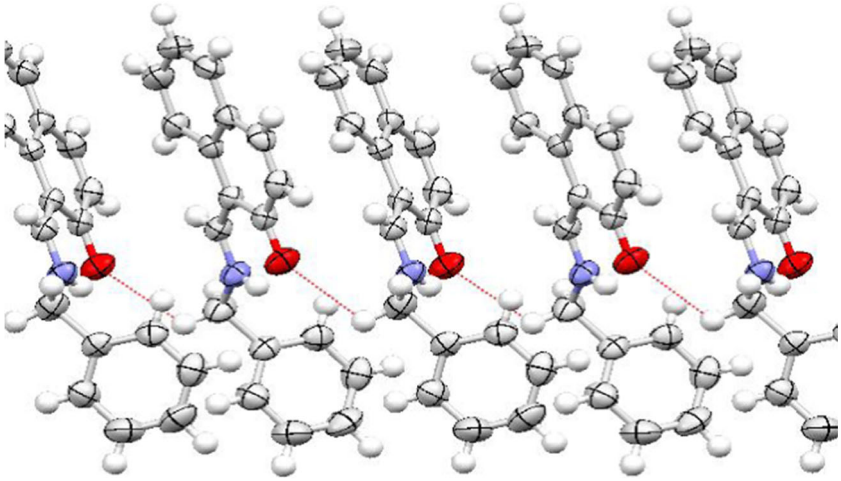

Fig. 3 Part of 3D network of chemosensor **R1** having Intramolecular hydrogen bonding

Preparation of Stock and Working Solutions of Metals and Chemosensor R1

For practical utilization and for detection of toxic metal ions in water samples it is very necessary for a chemosensor to work under aqueous condition. Chemosensor **R1** was not soluble in pure water. Therefore 0.001 M stock solution of chemosensor **R1** was prepared in pure DMSO. The chemosensor R1 was stable in DMSO. Working solutions were prepared by dilution of a stock solution in DMSO with a mixture of DMSO:H2O (20:80). Stock solutions of metal ions (0.01 M) were prepared in distilled water. Before spectroscopic analysis, test solutions were freshly prepared by appropriate dilution of stock solution to the corresponding desired concentration.

Metal Ion Binding Study by Fluorescence Spectroscopy

First the fluorescence of chemosensor **R1** 10 μM was investigated in mixed aqueous medium DMSO:H_2O (20:80) by taking 3 mL solution of it in a fluorometric cell. The fluorescence emission spectrum of this solution was taken upon excitation at 320 nm. Due to internal charge transfer its fluorescence emission was quenched and very weak fluorescence

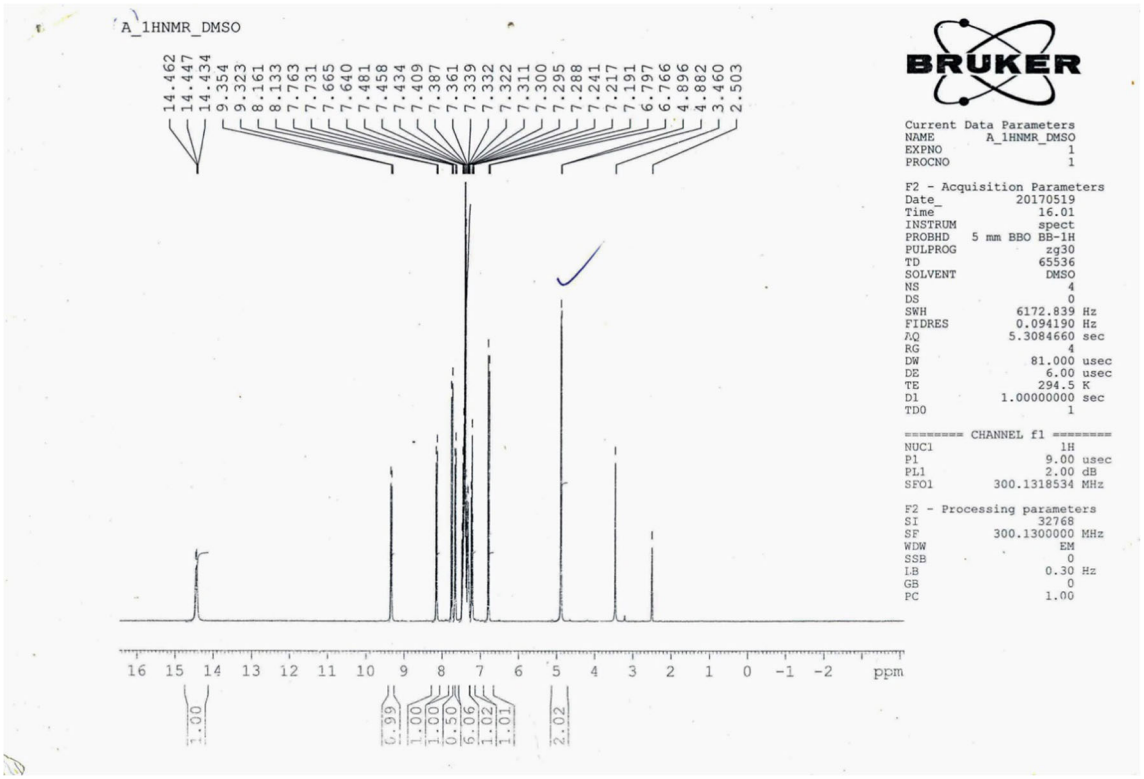

Fig. 4 ^{1}H NMR spectrum of chemosensor R1

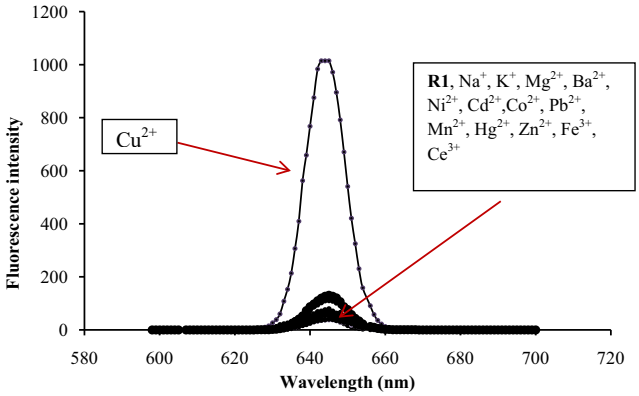

Fig. 5 Fluorescence emission spectrum of **R1** and relative fluorescence intensity changes upon the addition of monovalent (Na^+, K^+), divalent (Hg^{2+}, Zn^{2+}, Cd^{2+}, Pb^{2+}, Mn^{2+}, Co^{2+}, Ni^{2+}, Cu^{2+}) and trivalent cations (Ce^{3+}, Fe^{3+}, As^{3+}) as their aqueous solutions with an excitation at 320 nm, temp 25 °C

was observed at 645 nm. To investigate cation sensing ability of **R1**, 2 equiv. of Cu^{2+} and 20 equiv. of various alkali (Na^+, K^+), alkaline (Mg^{2+}, Ba^{2+}) transition metal ions (Ce^{3+}, Fe^{3+}, As^{3+}, Hg^{2+}, Zn^{2+}, Cd^{2+}, Pb^{2+}, Mn^{2+}, Co^{2+}, Ni^{2+}) were added separately to the solution of **R1** (2 mL). The mixture were allowed to equilibrate for 2 min at room temperature and then transferred separately into quartz cuvette and the fluorescence emission spectrum was monitored in the range 250–800 nm with an excitation at 320 nm and emission at 645 nm. The spectrum of all the examined metal ions was compared with the spectrum of **R1**. It was found that the non-fluorescence behavior become highly fluorescent only in the presence of Cu^{2+} ions and no detectable change in the fluorescence spectra was observed by other metal ions except a significant increase in the initial fluorescence intensity of **R1** only upon addition of Cu^{2+} as shown in Figs. 5 and 6. So among the tested metal ions only Cu^{2+} was the one that readily binds with **R1**. The increase in the fluorescence emission of **R1** can be explained on the basis of restriction of internal charge transfer (ICT) mechanisms. In the absence of Cu^{2+} ions, due to ICT mechanism, the fluorescence emission of the naphthalene fluorophore is greatly quenched. But in the presence of Cu^{2+} ions ICT phenomenon is restricted and fluorescence emission was considerably enhanced as result of rigid chelated complex formation [33].

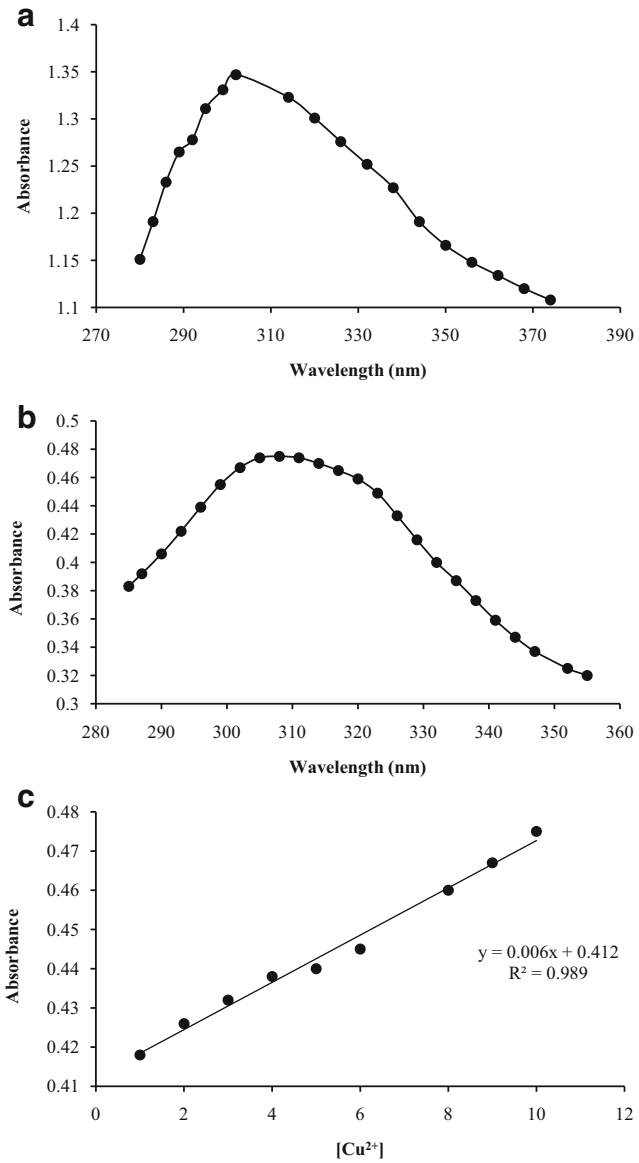

Fig. 7 **a** absorbance of 10 μM chemosensor **R1**. **b** Shifting of wavelength upon addition of Cu^{2+} ions, concentration of chemosensor R1 and Cu^{2+} ions is 10 μM. **c** Enhancement of absorbance at 308 nm upon addition of Cu^{2+} ions in the range 1–10 μM

UV-Visible Study

Since chemosensor R1 was not soluble in 100% aqueous media therefore DMSO was used as a cosolvent. UV-vis spectra of chemosensor R1 was taken in a mixed aqueous media in the absence and presence of

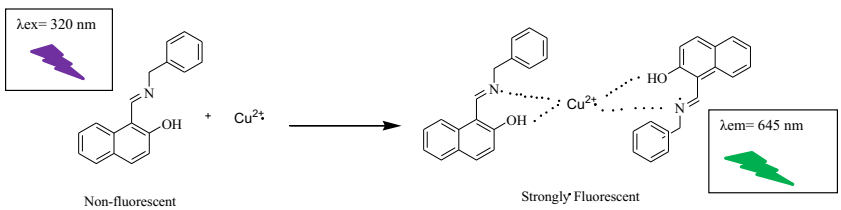

Fig. 6 Turn-On fluorescence behaviour of **R1** and the proposed binding mode and mechanism

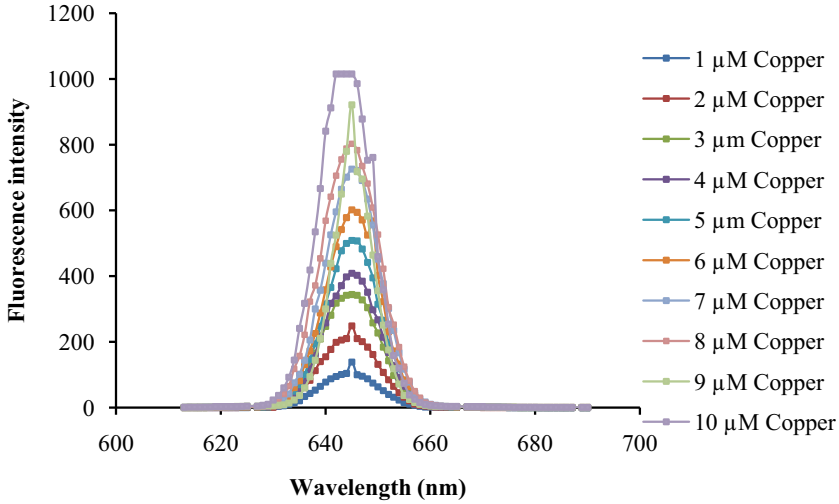

Fig. 8 Changes in the fluorescence emission spectra of chemosensor **R1** 10 µM with increasing amount of Cu^{2+} ion at 25 °C, λ_{ex} 320 nm, [Cu^{2+}] from left to right (1, 2, 3, 4, 5, 6, 7, 8, 9, 10 µM

different concentration of Cu^{2+} ions in distilled water. The UV-vis spectrum of chemosensor **R1** exhibited characteristic main absorption band in the range 260–380 nm with a λmax of 302 nm as shown in Fig. 7a. Upon addition of Cu^{2+} ions to chemosensor **R1** λ_{max} shifts to 308 nm. The red-shift of the λ_{max} is indicative of the coordination involving the hydroxyl and imine as a receptor and Cu^{2+} as an analyte. When various concentration Cu^{2+} ions were added to the solution of chemosensor **R1** the absorbance at 308 nm was enhanced as shown in the Fig. 7c. Test samples were prepared by using 10 µM solution of chemosensor **R1** and various concentrations of Cu^{2+} ions. All the measurements were made at room temperature.

Fluorogenic Detection of Cu^{2+}

To investigate the fluorescence-sensing behavior of chemosensor **R1**, a quantitative analysis of the binding affinity of chemosensor **R1** with Cu^{2+} ion was studied by fluorescence emission spectroscopy. To address the sensitivity, the fluorescence spectral properties of chemosensor **R1** were examined in DMSO:H_2O (20:80) as a function of concentration of Cu^{2+} ion added at room temperature. When excited at 320 nm the fluorescence emission spectrum of chemosensor **R1** displayed was very weak emission at 645 nm due to ICT mechanism in naphthalene moiety. However, the addition of Cu^{2+} ion in the range 1–10 µM led to a rapid increase in the fluorescence emission intensity at 645 nm as shown in Fig. 8 while no significant change in position of λ_{ex} and λ_{em} was observed. The enhancement of fluorescence was attributed to the restriction of ICT mechanism. The increase in fluorescence constitutes the basis for the detection of Cu^{2+} ion with the chemosensor **R1** proposed in this work. We also determined the linearity by plotting the emission intensity of chemosensor R1 at 645 nm as a function of the Cu^{2+} ion concentration in the range 1–10 µM. Chemosensor **R1** was sensitive to Cu^{2+} ion and the increase in fluorescence had a linear behaviour with correlation coefficient of $R^2 = 0.9978$ as shown in Fig. 9.

Detection Limit

The detection limit of chemosensor **R1** as a fluorescent sensor for the recognition of Cu^{2+} ion was determined from the plot

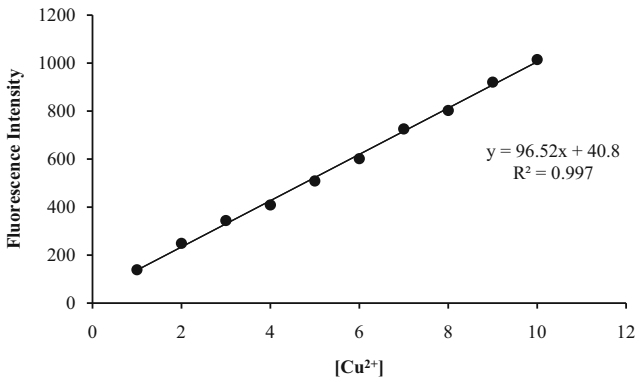

Fig. 9 Fluorescence emission profile of chemosensor R1 versus concentration of Cu^{2+} ion at 645 nm

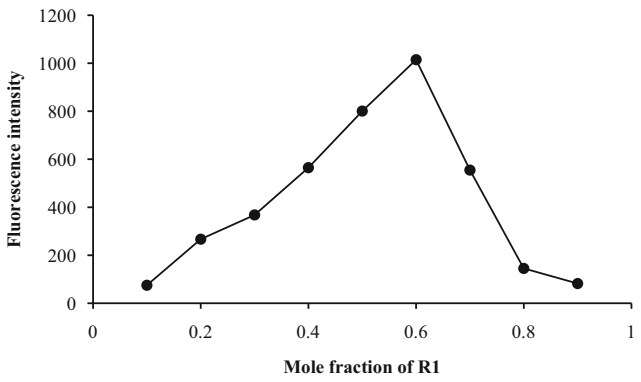

Fig. 10 Job's plot of **R1**-Cu^{2+} complex at 645 nm, [R1] + [Cu2+] = 10 µM, λ_{ex} is 320 nm, showing a binding stoichiometry of 2:1

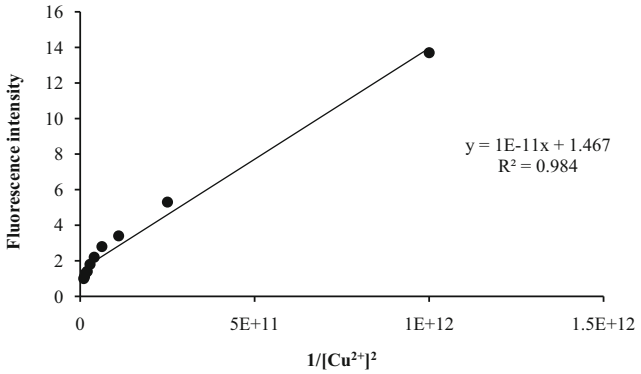

Fig. 11 Benesi-Hilderbrand plot for determination association constant of Cu^{2+} (1–10 μM) with chemosensor **R1**.The excitation wavelength is 320 nm and the emission wavelength is 645 nm

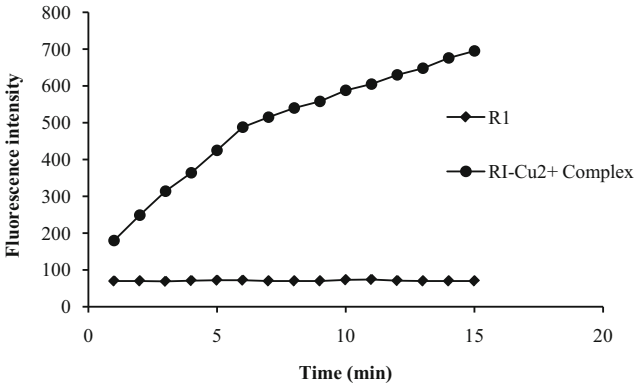

Fig. 13 Time dependent fluorescence emission intensity of chemosensor R1 in the absence and presence of Cu^{2+} at 645 nm, λex 320 nm

of fluorescence emission intensity as a function of Cu^{2+} ion concentration. The detection limit was calculated based on 3σ/k [41], where σ is the standard deviation of blank measurement and, and k is the slope of the plot. To determine σ, the fluorescence emission intensity of chemosensor **R1** was measured six times independently in the absence of copper ions. The detection limit calculated was found to be 30×10^{-9} M which is far below the WHO acceptable limit (30 μM or 1.5 mg/L of Cu^{2+}) in drinking water. The detection limit of the proposed chemosensor **R1** is lower than the fluorescent chemosensors of ref. [11, 42–45]. The detection limit was sufficiently low to recognize Cu^{2+} in nano molar range. In term of the detection limit and linear range it can be seen that the proposed sensor displays more sensitivity and selectivity for Cu^{2+} ion by fluorescence spectra.

Determination of Binding Stoichiometry and Association Constant

For determining the stoichiometry of chemosensor **R1** with Cu^{2+} ion the Job's plot experiment was undertaken in solution state using fluorescence spectroscopy. For spectroscopic analysis equimolar solutions of chemosensor **R1** and Cu^{2+} ion were prepared and mixed in different ratios by continuous increase of one constituent with the similar decrease of second constituent keeping total concentration constant. The sum of concentration of chemosensor **R1** and Cu^{2+} ion was kept constant at 10 μM according to the continuous variations, changing the mole fraction of chemosensor **R1** from 0.1 to 0.9 in a solution of [**R1**] + [Cu^{2+}]. Binding stoichiometry was determined by plotting the graph between the molar fraction of chemosensor **R1** and respective fluorescence emission intensity. When molar fraction reached to 0.6, maximum fluorescence emission was achieved at 645 nm, suggesting that the chemosensor **R1** and Cu^{2+} formed a 2:1 stoichiometry complex as shown in Fig. 10. It means one Cu^{2+} ion bind with two chemosensor **R1** molecules.

On the basis of 2:1 stoichiometry as determined by Job's plot the association constant was calculated with the help Benesi–Hildebrand plot from the increasing fluorescence emission intensity of chemosensor **R1** as a function of Cu^{2+} concentration. The association constant of the complex was calculated through the Benesi-Hildebrand equation stated below

$$\frac{F_{max-}F_o}{F-F_o} = 1 + \frac{1}{K\left[Cu^{2+}\right]^2} \quad (1)$$

Where Ka (M^{-2}) is an association constant. F_0 is the

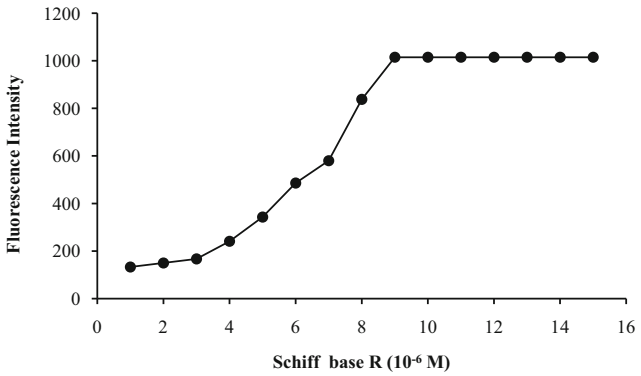

Fig. 12 Fluorescence emission intensity at 645 nm as a function of concentration of chemosensor **R1**. Copper concentration was kept constant (10×10^{-6} M)

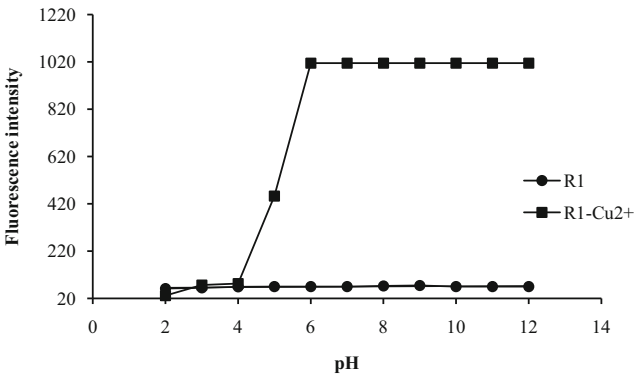

Fig. 14 Fluorescence response of chemosensor **R1** in the presence and absence of Cu^{2+} as a function of different pH values at room temperature, λ_{ex} is 320 nm and λ_{em} is 645 nm

fluorescence emission intensity of chemosensor R**1** in the absence of Cu^{2+}, F_{max} is the fluorescence emission intensity of chemosensor R**1** at [Cu^{2+}] in large excess and F is the fluorescence emission intensity obtained at different [Cu^{2+}] (λ_{ex} = 320 nm and λ_{em} = 645 nm. The association constant Ka was determined graphically by plotting F_{max}-F_0/F-F_0 versus 1/[Cu^{2+}] as shown in Fig. 11. According to the Eq. (1) data were linearly fitted showing a good liner relationship with slope (1×10^{-11}), and intercept = (1.4677) and confirming 2:1 complexation. The value of Ka value was determined from the slope and intercept of the line.

Effect of Chemosensor R1 Concentration on Fluorescence Response

The effect of an increasing concentration of chemosensor **R1** on fluorescence spectra of **R1**-Cu^{2+} complex was also investigated. Working solution for analysis were prepared in presence of Cu^{2+} ion (10 μM) by addition of various concentration of chemosensor **R1** solution in an incremental fashion in the range 1–15 μM. The fluorescence emission intensity of each sample was monitored separately at 645 nm and was plotted versus concentration of chemosensor **R1** as shown in Fig. 12. The fluorescence emission intensity enhanced gradually with increasing concentration of chemosensor **R1** but at higher concentration the fluorescence remain steady. Further replicate analyses were conducted to figure out reproducibility using constant concentration of chemosensor **R1** and Cu^{2+} ion (10 μM). Relative standard deviation (RSD) was 0.24% for 10 repeated fluorescence measurements.

Effect of Time

Response time is very important parameter of a fluorescence chemosensor therefore the kinetic studies of chemosensor **R1** (20 μM) both in the absence and presence of Cu^{2+} (2 μM) was investigated by fluorescence spectra. For this purpose the fluorescence emission intensities were measured at different interval of time. The time was varied in the range 1–15 min. In the absence of Cu^{2+} at 645 nm almost no changes in the fluorescence emission intensity of chemosensor **R1** was found as displayed in Fig. 13, demonstrating stability of chemosensor **R1** in the assay condition. In fluorescent spectroscopy long response time is undesired. The response of **R1** was almost instantaneous and fluorescence emission intensity turn on remarkably at 645 nm upon addition of aqueous solution of Cu^{2+} to solution of chemosensor **R1**, suggesting the rapid reaction of chemosensor **R1** with Cu^{2+}. For higher concentration of Cu^{2+} chemosensor **R1** has a fast response time of less than 30 s. This result indicates that the recognition was completed immediately without any detectable time delay after addition of Cu^{2+}. The chemosensor **R1** is highly suitable for real-time detection of Cu^{2+} in aqueous solutions in practical analysis.

Effect of pH

For practical utilization the effect of pH on the fluorescence emission intensity was investigated to determine a suitable pH range for sensing of chemosensor **R1** to Cu^{2+}. The fluorescence emission intensity measurements were performed in the absence and presence of 10 μM Cu^{2+}. The pH of the solutions was adjusted using HCl and NaOH and the alteration in fluorescence emission intensity at 645 nm was monitored in the pH range 2–12. The fluorescence emission intensity versus pH plot for the chemosensor **R1** and **R1**-Cu^{2+} complex is shown in Fig. 14. As shown in Fig, the fluorescence emission intensities of the metal free chemosensor **R1** remain unaffected in the pH range 2–12. This result indicate that the chemosensor **R1**, which is organic solvent-stable and also pH-stable, can be employed for recognition of Cu^{2+} as a useful potential fluorescent sensing material. After the addition of Cu^{2+} to the solution of chemosensor **R1** the fluorescence emission intensity at 645 nm rapidly enhanced in the pH range 5–12. As it is cleared from the Fig. 14, in the section of lower pH value (pH < 5) the emission intensity remain in the quenched state indicating poor stability of the **R1**-Cu^{2+} complexes at low pH. This is due to protonation on the chemosensor **R1** that prevents the formation of the **R1**-Cu^{2+} complex. The fluorescence emission intensity was in the turn-on state for pH > 5 indicating maximum complexation at high pH values and good fluorescence detection ability to Cu^{2+}.

Metal Ion Competition Experiment

Achieving high selectivity for a specific metal ion over a complex background of competitive metals is an important feature to evaluate the performance of a chemosensor. Therefore the suitability and practical applicability of chemosensor **R1** as a selective fluorescent probe for Cu^{2+} ion was checked by competition experiments in the presence of various metal ions. To investigate the interference from a number of cations the change in fluorescence emission intensity at 645 nm was recorded with solution of **R1** (20 μM) containing Na^{+}, K^{+}, Mg^{2+}, Ba^{2+}, Ce^{3+}, Fe^{3+}, As^{3+}, Hg^{2+}, Zn^{2+}, Cd^{2+}, Pb^{2+}, Mn^{2+}, Co^{2+}, Ni^{2+} (200 μM) and Hg^{2+}, Fe^{3+} (20 μM) followed by the addition of Cu^{2+} (20 μM). In recognition of Cu^{2+} with chemosensor **R1** no significant

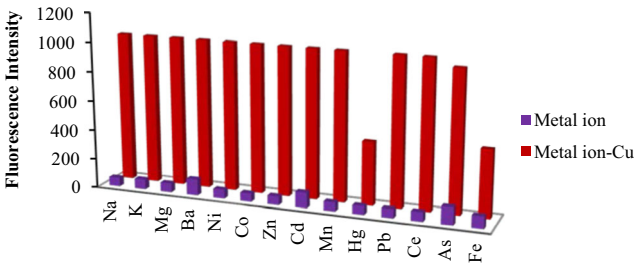

Fig. 15 Fluorescence response of **R1** to 200 μM various tested metal ions (grey bar) and to the mixture of 200 μM tested metal ions with 20 μM Cu^{2+} (black bar) at room temperature, λ_{ex} = 320 nm

Table 3 Comparison of R1 with previous work [19, 20, 24, 42, 46, 47]

Structure of sensor	Fluorophore	Analyte	Detection mode/ remarks	Testing media	Detection limit M	Optimal pH range	Ref
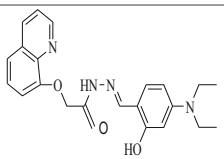	Quinoline	Cu^{2+}	Quenching λex/λem= 399/514 Red shift and fluorogenic change	Tris–HCl solution [V(C2H5OH)/V(H2O)= 5:5, pH=7.2]	6.66×10^{-8} M	NA	19
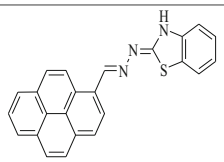	Pyrene	Cu^{2+}	Enhancement λex/λem= 385/468 Chromo- and fluorogenic changes	Acetonitrile–water (v/v = 3/1, 5 mM HEPES, pH 7.0)	2.73×10^{-6} M	2-8.5	20
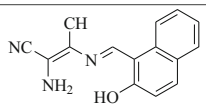	Naphthalene	Cu^{2+}, cystein	Enhancement (UV-vis) λ_{max}= 489	10 mM bis-tris buffer/DMSO (7:3, v/v) Bathochromic shift and chromogenic change	2.4×10^{-6} M	5-10	24
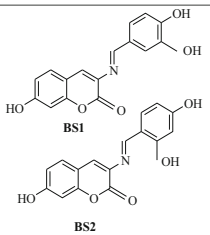	Coumarin	Cu^{2+}, Fe^{3+}	Quenching λex/λem= 340, 364/458, 437/ Change in fluorescence	Aqueous solution (30 mM HEPES buffer, pH 7.4, 1% DMSO)	1.27×10^{-4} M, 1.04×10^{-4} M	NA	43
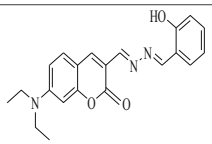	Coumarin	Cu^{2+}	Quenching λex/λem= 467/537 Chromo- and fluorogenic change	Methanol–water (v/v = 1 : 1, 10 mM HEPES, pH 7.0)	0.27×10^{-6} M	5-9	47
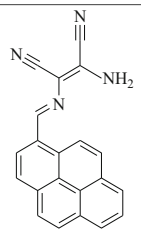	Pyrene	Cu^{2+}	Enhancement λex/λem= 350/417 Chromo- and fluorogenic change	Acetonitrile-water (v/v= 1:1, 10 mM HEPES, pH=7.0)	NA	5.5-7.5	48
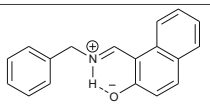	Naphthalene	Cu^{2+}	Enhancement λex/λem= 320/645 nm Fluorogenic change	DMSO: H_2O (2:8)	30×10^{-9} M	5-12	This work

interference was observed in the presence of most competitive metal ions except for the Hg^{2+} and Fe^{3+} ion as shown in the Fig. 15. This indicates that only Hg^{2+} and Fe^{3+} compete with Cu^{2+} for binding with chemosensor **R1**. The fluorescence enhancement caused by the Cu^{2+} ion remained unaffected with most examined metal ions. These observations suggests that **R1** can be applied as an outstanding selective and sensitive fluorescent chemosensors for estimation of trace amount of Cu^{2+} ion in real samples in the presence of these metals ions.

Comparison with Pervious Works

Specific features of the proposed chemosensor **R1** towards Cu^{2+} was compared with some previously reported chemosensor for Cu^{2+} in Table 3.

Most of the chemosensor required rigorous testing media and most of them displayed quenching of fluorescence upon interaction with Cu^{2+}. Our proposed chemosensor R1 presents a number of attractive analytical features such as one step synthesis, high selectivity for Cu^{2+}, sensitivity, enhancement of fluorescence, good reproducibility, wide pH range and can be used for the rapid detection of Cu^{2+} in natural water samples.

Reversibility of Chemosensor R1

In the development of fluorescent chemosensor, the main feature to increase their applicability is the detection. The use of a chemosensor for detection of particular metal ion, reversibility is an important aspect in practical applications. To investigate whether the enhancement of fluorescence emission intensity was as a result of indeed Cu^{2+} ion binding with chemosensor **R1** and not photoactivation of chemosensor **R1** or a chemical reaction reversibility experiment was conducted to study whether the complexation of chemosensor **R1** with Cu^{2+} is reversible or not. For this purpose we use a strong metal ion chelator EDTA to revert the fluorescence. To the solution containing **R1**-Cu^{2+} complex 1 equiv. of EDTA was introduced and its fluorescence emission intensity was monitored at 645 nm after interaction with EDTA. After the addition of EDTA fluorescence emission signal was restored at 645 nm. This analysis suggests that the complexation between copper and chemosensor **R1** is really and chemically reversible as shown in Fig. 16.

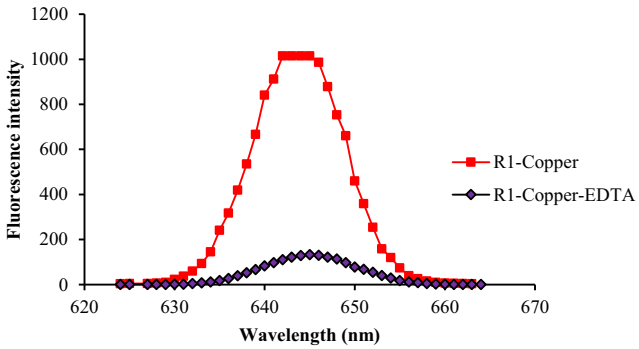

Fig. 16 Reversibility of binding interaction between chemosensor **R1** (10 μM) and copper (20 μM) by the introduction of EDTA (20 μM) to the solution of complex

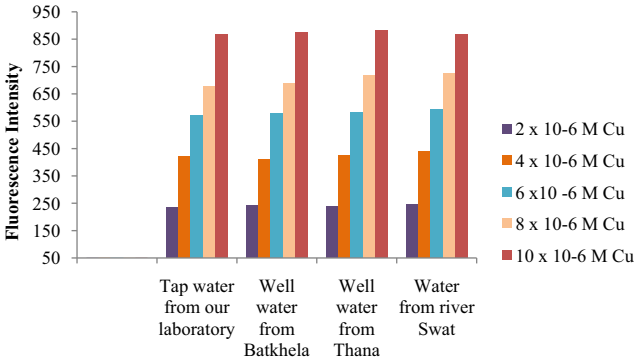

Fig. 17 Respective fluorescence responses of chemosensor **R1** to Cu^{2+} ion added to the natural water samples at room temperature, [Cu^{2+}] 2–10 μM, λ_{ex} is 320 nm and λ_{em} is 645 nm, [R1] 10 μM

Application to the Analysis of Natural Water Samples

To investigate the practical applicability and sensitivity of the new chemosensor R1 in complex matrices, we examined the ability of chemosensor **R1** to detect trace amount of Cu^{2+} ions in three natural water samples using the spike method. Chemosensor **R1** was sensitive enough to detect Cu^{2+} ion in natural water samples. For this purpose samples were collected from three significantly different sourcses: the river water from river Swat, tap water from laboratory water pipe located at university of Malakand KPK and well water from Batkhela and Thana. Different concentrations of Cu^{2+} ion were added into the water samples and assayed within 24 h of the collection. The fluorescence emission intensity of each sample was monitored at 645 nm and the results are shown in the Fig. 17. As it is cleared from the Figure that fluorescence emission intensity of chemosensor **R1** was proportional to the amount of Cu^{2+} ion added. These results displayed that relative to distilled water chemosensor **R1** can also detect Cu^{2+} ion in the complex media, pointing out its potential applicability in the field of toxicology and environment sciences.

Conclusion

In conclusion, we have developed a Schiff based fluorescent chemosensor for Cu^{2+} ion and it was characterized by FTIR and single X-ray diffraction and ^1H NMR. Significant fluorescence enhancement was observed by this sensor only in the

presence of Cu2+ ion. The enhancement was due to the restriction of ICT phenomenon. The optimal pH range for detection of Cu^{2+} ion was 5–12. Our proposed chemosensor **R1** possess high selectivity, sensitivity, and fast response time towards Cu^{2+} ion over a large number of competing metal ions. The excellent low limit of detection of this chemosensor **R1** towards Cu^{2+} ion can be useful in detection of trace amount of Cu^{2+} ion in environmental samples. The response was reversible and the given sensor was successfully applied for the detection of Cu2+ in natural water sample.

References

1. Ivo G, Jean-Marc C, Valmadimir B (2004) New green fluorescent polyvinylcarbazole copolymer with 1,8-naphthalimide side chains as chemosensor for iron cations. Polym Adv Technol 15:382–386
2. Zhanxian L, Lifeng Z, Xiaoya L, Yonghai N, Jianhong C, Liube W, Mingming Y (2012) A fluorescent color/intensity changed chemosensor for Fe^{3+} by photo induced electron transfer (PET) inhibition of fluoranthene derivative. Dyes Pigments 94:60–65
3. Mani V, Shu-Pao W (2012) A BODIPY-based colorimetric and fluorometric chemosensor for Hg (II) ions and its application to living cell imaging. Org Biomol Chem 10:5410–5416
4. Li J, Ling W, Bo Z, Rui-Yong W, Gui Y (2011) A fluorescence turn-on Hg^{2+} probe based on rhodamine with excellent sensitivity and selectivity in living cells. Open J Inorg Chem 1:16–22
5. Ghandhi S, Thangaraj A, Durajsamy C (2012) Development of a pyrene based "turn on" fluorescent chemosensor for Hg^{2+}. RSC Adv 2:10605–10609
6. Qianni G, Qingbin Z, Xiaoxiao Z, Xin Z (2014) Highly sensitive detection of mercury (II) in aqueous media by tetraphenylporphyrin with a metal ion receptor. Supramol Chem 26:836–842
7. Arunabha T, Dipendu M, Pranab D, Bijan M, Sundargopal G (2014) Synthesis of triazole linked fluorescent amino acid and carbohydrate bio-conjugates: a highly sensitive and skeleton selective multi-responsive chemosensor for Cu (II) and Pb (II)/Hg (II) ions. RSC Adv 4:1918–1928
8. Keyur DB, Hrishikesh SG, Bharat AM, Disha JV, Debdeep M, Vinod KJ (2012) Calix receptor edifice; scrupulous turn off fluorescent sensor for Fe (III), Co (II) and Cu (II). J Fluoresc 22:1493–1500
9. Shi-Rong L, Shu-Pao W (2011) An NBD-based sensitive and selective fluorescent sensor for copper (II) ion. J Fluoresc 21:1599–1605
10. Zhihong X, Like Z, Rui G, Tiancheng X, Chanzeng W, Zhi Z, Fengling Y (2011) A highly sensitive and selective colorimetric and off–on fluorescent chemosensor for Cu^{2+} based on rhodamine B derivative. Sensors Actuators B Chem 156:546–552
11. Muhammad S, Ki-Hwan L (2014) Selective fluorescence detection of Cu^{2+} in aqueous solution and living cells. J Lumin 145:843–848
12. Rakesh KM, Pallavi S (2007) Novel copper (II)-selective electrode based on 2,2′: 5′,2″-terthiophene in PVC matrix. Int J Electrochem Sci 2:832–847
13. Najua DT, Luqman AC, Zwani Z, Suraya AR (2008) Adsorption of copper from aqueous solutions by elais guineensis kernel activated carbon. J Eng Sci Technol 3:180–189
14. Aeju L, Jungwook C, Ok PK, Hyunjin C, Jin WK, Soo-Young Y, Kyeongsoon P (2013) A novel near-infrared fluorescence chemosensor for copper ion detection using click ligation and energy transfer. Chem Commun 49:5969–5971
15. Yeong KJ, Chang UN, Ha LK, In HH, Cheal K (2013) A Selective colorimetric and fluorescent chemosensor based-on naphthol for detection of Al^{3+} and Cu^{2+}. Dyes Pigments 99:6–13
16. Cesar GF (2005) Relevance, essentiality and toxicity of trace elements in human health. Mol Asp Med 26:235–244
17. Selvaraj R, Younghun K, Cheol KJ, Jongheop Y (2004) Removal of copper from aqueous solutions by aminated and protonated mesoporous aluminas: kinetics and equilibrium. J Colloid Interface Sci 273:14–21
18. Pragnesh ND, Subrahmanyam N, Surendra S (2009) Kinetics and thermodynamics of copper ions removal from aqueous solution by use of activated charcoal. Indian J chem Technol 16:234–239
19. Chen Z, Yan S, Ning X, Yapeng L, Jiayuan X (2014) A novel highly sensitive and selective fluorescent sensor for imaging copper (II) in living cells. J Fluoresc 24:1331–1336
20. Hsuan-Fu W, Shu-Pao W (2013) A Pyrene-based highly selective turn-on fluorescent sensor for copper (II) ions and its application in living cell imaging. Sensors Actuators B 181:743–748
21. Tae GJ, Yu JN, Jae JL, Myoung ML, Sun YL, Cheal K (2015) A diaminomaleonitrile based selective colorimetric chemosensor for copper (II) and fluoride ions. New J Chem 39:2580–2587
22. Juanmei Z, Li Z, Wenjing L, Dozhong S, Rilong Z, Dawei P (2011) Determination of trace copper in water samples by anodic stripping voltammetry at gold microelectrode. Int J Electrochem Sci 6:4690–4699
23. Jafer Ahmad A, Shajudha Begum A (2012) Adsorption of copper from aqueous solution by low cost adsorbent. Arch Appl Sci Res 4:1532–1539
24. Seul AL, Jae JL, Jong WS, Kil SM, Cheal K (2015) A colorimetric chemosensor for the sequential detection of copper (II) and cysteine. Dyes Pigments 116:131–138
25. I-Ting H, Jean-Ho C, Wen-Sheng C (2011) Calix[4] arene with lower-rim β-amino α,β-unsaturated ketones containing bis-chelating sites as a highly selective fluorescence turn-On chemosensor for two copper (II) ions. Eur J Org Chem 2011:1472–1481
26. Shu-Pao W, Zhen-Ming H, Shi-Rong L, Peter KC (2012) A pyrene-based highly selective turn-on fluorescent sensor for copper (II) ion and its application in live cell imaging. J Fluoresc 22:253–259
27. Manoj K, Nagendra B, Vandana B (2010) Fluorescent chemosensor for Cu^{2+} ion based on iminoanthryl appended calix[4]arene. J Incl Phenom Macrocycl Chem 66:139–145
28. Muthaiah S, Yen-Hsing W, Ashutosh S, Mandapati VRR, Hong-Cheu L (2013) Novel pyrene- and anthracene-based Schiff base derivatives as Cu^{2+} and Fe^{3+} fluorescence turn-on sensors and for aggregation induced emissions. J Mater Chem A 1:1310–1318
29. Nur A, Emu H, Ibrahim Y, Alaaddin C (2009) A highly sensitive and selective fluorescent sensor for the determination of copper (II) based on a schiff base. Dyes Pigments 83:211–217
30. Aixiang D, Fang T, Tao W, Xutang T, Jiaxizng Y (2015) A α-cyanostilbene-modified Schiff base as efficient turn-on fluorescent chemosensor for Zn^{2+}. J Chem Sci 127:375–382
31. Dehua Z, Xiaoyan Z (2013) Crystallization and characterization of a new fluorescent molecule based on Schiff base. JCPT 3:28–30
32. Lei L, Yong-Qiang D, Hong-Wei L, Wa B, Yuqing W (2010) Fluorescent chemosensor based on Schiff base for selective detection of zinc (II) in aqueous solution. Tetrahedron Lett 51:618–621
33. Supriti S, Titas M, Basab C, Anuradha M, Anupam B, Jaromir M, Pabitra C (2012) A water soluble Al^{3+} selective colorimetric and fluorescent turn-on chemosensor and its application in living cell imaging. Analyst 137:3975–3981
34. Mohamed NI, Salah EAS (2007) Synthesis, characterization and use of Schiff bases as fluorimetric analytical reagents. E-J Chem 4:531–535

35. Vinod KG, Ashok KS, Lokesh KK (2014) A turn-on fluorescent chemosensor for Zn2+ions based on antipyrine schiff base. Sensors Actuators B Chem 204:507–514
36. Reza A, Tayebe A, Hassan K, Majid R (2013) A new asymmetric Schiff base system as fluorescent chemosensor for Al^{3+} ion. Inorg Chem Commun 33:63–67
37. Xavier A, Srividhya N (2014) Synthesis and study of Schiff base ligand. IOSR-J Appl Chem 17:6–15
38. Vinod KG, Sudhir KS, Lokesh KK, Ajay KJ (2015) A highly selective colorimetric and turn-on fluorescent chemosensor based on 1-(2-pyridylazo)-2-naphthol for the detection of aluminium (III) ions. Sensors Actuators B Chem 209:15–24
39. Sheldrick GM (2008) A short history of SHELXL. Acta Crystallogr A 64:112–122
40. Westrip SP (2010) PublCIF: software for editing, validating and formatting crystallographic information files. J Appl Crystallogr 43:920–925
41. Zhiyuan Z, Chunming S, Aifeng L, Zhenyu Z, Dongmei Z (2015) Highly selective detection of Cr (VI) in water matrix by a simple 1, 8-Naphthalimide-based turn-on fluorescent sensor. J Fluoresc 25: 335–340
42. Olimpo G-B, Bruce KC, Claudio P, Natalia M, Marco TN, Natalia PM, Paulina P, Margarita EA (2014) Coumarin-based fluorescent probes for dual recognition of copper (II) and iron (III) ions and their application in bio-imaging. Sensors 14:1358–1371
43. Hyo SJ, Pil SK, Jeong WL, Jae IK, Chang SH, Jong WK, Shihai Y, Jin YL, Jung HL, Taiha J, Jong SK (2009) Coumarin-derived Cu^{2+}-selective fluorescence sensor: synthesis, mechanisms, and applications in living cells. J Am Chem Soc 131:2008–2012
44. Chunwei Y, Lingxin C, Jun Z, Jinhua L, Ping L, Wenhai W, Bing Y (2011) "Off-On" based fluorescent chemosensor for Cu2+ in aqueous media and living cells. Talanta 85:1627–1633
45. Yan-Qin W, Ying-Lai T, Fan Y, Yong-Rui Z, Bao-Hui Y (2007) A new selective fluorescent chemosensor for Cu (II) ion based on zinc porphyrin-dipyridylamino. Inorg Chem Commun 10:443–446
46. Jiun-Ting Y, Wei-Chieh C, Shi-Rong L, Shu-Pao W (2014) A coumarin-based sensitive and selective fluorescent sensor for copper (II) ions. New J Chem 38:4434–4439
47. Shu-Pao W, Tzu-Hao W, Shi-Rong L (2010) A highly selective turn-on fluorescent chemosensor for copper (II) ion. Tetrahedron 66:9655–9658